



Published in final edited form as:

*Anal Chem.* 2009 February 15; 81(4): 1347–1356. doi:10.1021/ac801883k.

## Non-Covalent Protein Tetramers and Pentamers with “n” Charges Yield Monomers with n/4 and n/5 Charges

Richard L. Beardsley<sup>‡,1</sup>, Christopher M. Jones<sup>‡</sup>, Asiri S. Galhena<sup>2</sup>, and Vicki H. Wysocki  
Department of Chemistry, University of Arizona, 1306 E. University Blvd., PO Box 210041,  
Tucson, AZ

### Abstract

In recent years mass spectrometry based techniques have emerged as structural biology tools for the characterization of macromolecular, non-covalent assemblies. Many of these efforts involve preservation of intact protein complexes within the mass spectrometer, providing molecular weight measurements that allow the determination of subunit stoichiometry and real-time monitoring of protein interactions. Attempts have been made to further elucidate subunit architecture through the dissociation of subunits from the intact complex by colliding it into inert gas atoms such as argon or xenon. Unfortunately, the amount of structural information that can be derived from such strategies is limited by the nearly ubiquitous ejection of a single, unfolded subunit. Here, we present results from the gas-phase dissociation of protein-protein complexes upon collision into a surface. Dissociation of a series of tetrameric and pentameric proteins demonstrate that alternative subunit fragments, not observed through multiple collisions with gas atoms, can be generated through surface collision. Evidence is presented for the retention of individual subunit structure, and in some cases, retention of non-covalent interactions between subunits and ligands. We attribute these differences to the rapid large energy input of ion-surface collisions, which leads to the dissociation of subunits prior to the unfolding of individual monomers.

### Introduction

Since Theodor Svedberg's landmark invention of the analytical ultracentrifuge first revealed that proteins can consist of more than one polypeptide chain, the stoichiometry and quaternary arrangement of subunits has become essential to the definition of protein structure.<sup>1</sup> We now realize that proteins often function in large assemblies, making it paramount that these molecules be understood in the context of the various ligands to which they bind (i.e., other proteins, oligonucleotides, and small molecules). Biophysical methods for characterizing macromolecular assemblies have primarily been the domain of x-ray crystallography, NMR, and electron microscopy, but mass spectrometry has recently emerged as powerful structural biology tool in its own right. Fifteen years ago, it was demonstrated that non-covalently bound proteins could be preserved within the mass spectrometer, and that these complexes reflected the biologically specific interactions that existed among protein subunits.<sup>2–4</sup> Mass spectrometry has since evolved from the simple mass measurement of non-covalently bound species, into a robust technology capable of discovering novel protein-protein interactions,<sup>5</sup> identifying ligand binding sites,<sup>6</sup> probing substrate-specific conformational changes,<sup>7</sup> and monitoring dynamic binding events.<sup>8,9</sup>

Correspondence to: Vicki H. Wysocki.

<sup>‡</sup>These authors contributed equally to this work.

<sup>1</sup>Present address: Hoffmann-la Roche, 340 Kingsland St. Nutley, NJ 07110

<sup>2</sup>Present address: Georgia Institute of Technology, 901 Atlantic Drive NW, Atlanta, GA 30332

Recently, efforts to elucidate the arrangement of proteins within multimeric complexes have added a powerful new dimension to MS as a structural biology approach. Most of these methods have relied on chemical cross-linking,<sup>10, 11</sup> or partial solution-phase denaturation,<sup>11–13</sup> followed by MS to identify spatially proximate subunits. In theory, the direct gas-phase dissociation of intact macromolecules should also provide insights into their subunit architecture, avoiding any prior tedious and time-consuming solution-phase chemistry. In tandem mass spectrometry (MS/MS), a molecular ion of interest can be mass selected and fragmented, and the resulting fragment ions can provide additional structural information about the original precursor ion. Gas-phase dissociation experiments have enhanced the structural analysis of biological molecules such as DNA,<sup>14</sup> carbohydrates,<sup>15</sup> and individual proteins.<sup>16</sup>

Smith and coworkers were the first to fragment protein multimers in the gas-phase when they investigated a series of biologically specific tetramers.<sup>17, 18</sup> Gas-phase dissociation of these tetramers produced exclusively monomer and trimer fragment ions, products not reflective of the strong dimer-dimer interactions observed in solution. It is now known that MS/MS of multimeric proteins, with few published exceptions,<sup>19</sup> leads primarily to the ejection of a single, highly charged monomer, regardless of the protein size, structure, or subunit composition. The number of charges retained by the monomer is significant as it provides insight into the conformation of the product ion. It is well known that the multiply charged ions produced by electrospray reflect protein structure, with denatured proteins accommodating more charge than compact, folded conformations.<sup>20–22</sup> Similarly, several research groups have concluded that a protein with “n” subunits dissociates through the unfolding of a single monomer, presumably to relieve Coulomb repulsion within the multiply charged intact complex.<sup>17, 23–27</sup> The increase in surface area is accompanied by considerable charge enrichment of the unfolded monomer such that the ejected subunit absconds with a disproportionate share of the charge with respect to its relative mass. A more folded (n-1)-mer is left with the remainder of the charge resulting in charge partitioning that is highly asymmetric with respect to the mass of each product, but symmetric in terms of their surface areas.<sup>26, 27</sup> With few exceptions,<sup>19</sup> this effect is ubiquitous, having been observed with complexes as small as dimeric cytochrome *c*<sup>24, 25, 28</sup> and as large as the 800 kDa tetradecamer of chaperonin GroEL.<sup>7, 29</sup> The consequence of this general dissociation mechanism is that little structural information on the arrangement of subunits within the complex can be derived from their tandem mass spectra. While some gas-phase dissociation experiments have provided limited spatial information for weakly bound proteins or proteins on the periphery of a complex,<sup>30, 31</sup> a comprehensive picture of the overall subunit architecture remains elusive. The interpretation of protein quaternary structure by mass spectrometry would be greatly facilitated if larger, structurally significant subcomplexes could be observed directly from the gas-phase dissociation of the intact complex.

One way to overcome this problem may be through alternative means of activating protein complexes, allowing access to dissociation channels other than the ejection of a single, unfolded monomer. Currently, the predominant method of dissociating protein complexes is through collision-induced dissociation (CID). In CID, the projectile ions are accelerated into inert gas atoms (i.e. argon or xenon) to provide collisions that convert the precursor ion kinetic energy into internal vibrational modes, leading to unimolecular decay. As a protein complex often carries a high net charge, its laboratory frame kinetic energy will typically be several thousand electron volts (eV) during a CID experiment. Despite this high kinetic energy, the number of collisions necessary for dissociation of a protein complex may still number in the tens of thousands as conversion of that energy into internal modes of the protein is highly inefficient due to the relative size of the protein ion and the collision gas. Alternatively, the use of a more massive collision target, such as a surface, can offer more

efficient energy transfer, activating ions on a much shorter time frame (picoseconds rather than microseconds). Previous work in our group indicated that surface-induced dissociation (SID) may provide the ability to dissociate intact protein complexes without significant monomer unfolding.<sup>32</sup> In that study, non-specific dimers of cytochrome c were investigated by SID and CID in a modified quadrupole time-of-flight (Q-TOF) mass spectrometer.<sup>33</sup> Collision of the dimers with 11 charges into a fluorinated self-assembled monolayer (FSAM) covalently bound to a gold surface, produced monomer fragments with five and six charges, as opposed to the highly asymmetric charge partitioning (8+/3+) observed by gaseous collisions. The charge equivalence of the monomer fragment ions suggested that the two subunits dissociate from the dimeric complex with similar conformations rather than through the unfolding of one of the monomers.

In the present study, we investigate the dissociation of several tetrameric and pentameric protein complexes by comparing the effects on dissociation pathways induced by either a single surface collision event (SID) or multiple collisions with neutral gas atoms (CID). It is demonstrated that tetrameric and pentameric protein complexes dissociate via charge-symmetric pathways during SID, unlike the asymmetric behavior observed during CID experiments. Based on these observations we propose that the dissociation of protein complexes following a surface collision must proceed through a relatively folded transition state, and is affected by the internal energy of the activated ion. Furthermore, disruption of protein complex structure (i.e. unfolding of protein subunits) prior to surface collision leads to more asymmetric pathways suggesting that dissociation likely occurs faster than large-scale protein structural rearrangement.

## Experimental Methods

### Materials

Transthyretin (Prealbumin from human plasma) was purchased as lyophilized powder from Sigma-Aldrich Co. (St. Louis, MO). Human hemoglobin was purchased from Sigma-Aldrich Co. for the ion mobility experiments and prepared from fresh hemolysate of a healthy adult male for CID and SID experiments. Recombinant human C-reactive protein, expressed in *E. Coli* was purchased from EMD Chemicals, Calbiochem product brand (Gibbstown, NJ). Ammonium acetate was purchased from Spectrum Chemicals & Laboratory Products (Gardena, CA). Micro Bio-spin columns for buffer exchange were purchased from Bio-Rad (Hercules, CA). Gold surfaces were purchased from Evaporated Metal Films (Ithaca, NY) and 2-(perfluorooctyl)-ethanethiol was synthesized from the corresponding iodide and thiourea by the Chemical Synthesis Facility at the University of Arizona as described previously.<sup>34</sup>

### FSAM Surfaces

18 mm × 12 mm glass surfaces coated with a 10 Å layer of titanium followed by a 100 Å layer of gold and formation of a fluorinated self-assembled monolayer (FSAM) surface were employed as SID targets. The gold was chemically modified in-house with a self-assembled monolayer of 2-(perfluorooctyl)-ethanethiol to reduce neutralization and enhance energy transfer efficiency. The gold surfaces were first UV-cleaned for 15 minutes (Boekel Industries Inc., Feasterville, PA), followed by incubation in a 1mM ethanolic solution of 2-(perfluorooctyl)-ethanethiol for a period of 24–72 hours. After incubation, the surface was sonicated in ethanol five times prior to insertion into the instrument.

### Mass Spectrometry

Proteins were buffer exchanged into 200 mM ammonium acetate (pH 7) using microcentrifuge columns, or dissolved directly into ammonium acetate. Aqueous protein

solutions were loaded into glass capillaries pulled in-house with a P-97 micropipette puller (Sutter Instruments, Hercules, CA). Proteins were then electrosprayed via a home-built nanoESI source by inserting a metal wire into the back of the glass capillary and applying voltages between 1.3–1.8 kV. All experiments were conducted on a modified Q-TOF 2 mass spectrometer (Waters Corp., Milford, MA) that has been described elsewhere.<sup>33</sup> Briefly, an in-line SID device was installed in between the quadrupole mass analyzer and gas collision cell to allow direct comparisons of CID and SID on the same instrument. The SID device, which includes a surface holder, ion beam deflectors and focusing lenses, is 45 mm in length, and was inserted by removing the transport hexapole following the collision cell. The collision cell was moved closer to the entrance of the TOF to make room for the SID device. The instrument can be operated in two modes; one that allows deflection of the ion beam into the surface for SID experiments, or alternatively, a bypass mode in which ions are transmitted through the apparatus without hitting the surface for single-stage MS and CID experiments. This allows direct comparison between the two ion activation methods in the same instrument and over similar observation time frames.

Mass spectra were acquired under conditions optimized for the transmission of non-covalent protein complexes. Pressure in the source region of the instrument was raised by partially restricting the vacuum line to the rotary pump as described previously.<sup>35</sup> Ions were selected for tandem mass spectrometry experiments with an extended mass range quadrupole and accelerated into either the surface or the gas-filled hexapole collision cell. The collision cell was operated either without Ar gas, using the collision cell solely as a hexapole ion guide to gauge the effects of SID alone with minimal gas collisions, or with Ar gas to test the necessity of collisional focusing of high  $m/z$  product ions following surface collision. For the systems studied here, the presence of gas in the collision cell was observed to have minimal influence on the appearance of the SID product ion spectrum, although we have observed benefits of using gas in the study of larger protein complexes.<sup>36</sup> For CID experiments, the collision cell pressure was measured in the quadrupole analyzer chamber and typically maintained between  $1\text{--}6 \times 10^{-4}$  mbar. For CID, the laboratory collision energy is described by the DC offset between the source hexapole and the grounded collision cell ( $\Delta V_{\text{source-gas cell}}$ ) multiplied by the charge state of the precursor ion. For SID it is defined as the product of the DC offset between the hexapole and the *surface* ( $\Delta V_{\text{source-surface}}$ ) and the precursor ion charge state, with the surface typically held at +10 volts. Product ions formed by CID and SID activation were measured by the TOF analyzer.

### Simulated Spectra

Simulated tandem mass spectra were generated using Microcal Origin Version 6.0 in a manner similar to that described by Aquilina et al.<sup>37</sup> Three parameter Gaussian curves were plotted for the individual peaks of each oligomer population based on the  $m/z$  ratio, intensity and width of each peak from the experimental data. The contributions of each oligomer population were then added to give a simulated spectrum for all product ions.

### Results and Discussion

A series of tetrameric and pentameric protein complexes were fragmented by tandem mass spectrometry using either argon gas or a fluorinated SAM surface as the collision target. Preliminary results for the fragmentation of multi-subunit complexes via surface collision have been previously published by our group,<sup>36, 38</sup> but here we present a more thorough investigation into their dissociation, including studies of homo- and hetero-oligomeric complexes, energy-resolved surface-induced dissociation, and the influence of protein conformation prior to surface collision. We also expand upon the mechanism proposed in our previous communication<sup>32</sup> to explain differences observed in the product ion spectra when colliding oligomeric proteins into a surface rather than gas atoms.

## Comparison of CID and SID of Homotetrameric Transthyretin

Transthyretin, a protein that forms non-covalent complexes composed of four identical ~13.5 kDa subunits, was used to probe the dissociation products generated by surface collision. The gas phase dissociation behavior of this complex has been previously investigated by Robinson and coworkers through collisions with argon in a Q-TOF mass spectrometer.<sup>39</sup> The CID fragmentation of this non-covalent assembly is thus well characterized, making it a suitable model system for the evaluation of SID of multimeric complexes. Figure 1 displays the dissociation of the 15+ charge state of this tetramer through multiple argon collisions in the collision cell (**1a**) and collision into an FSAM surface (**1b**). Both spectra were acquired on our modified Q-TOF with the surface assembly installed. The spectra displayed in Figure 1 were acquired at laboratory collision energies of 1350 eV [ $(\Delta V_{\text{source-gas cell}} = 90 \text{ V}) \times 15+ \text{ charge state}$ ] and 750 eV [ $(\Delta V_{\text{source-surface}} = 50 \text{ V}) \times 15+ \text{ charge state}$ ], for CID and SID respectively. These collision energies were chosen for comparison because the survival of the precursor ion is similar in each case.

It is immediately apparent from these spectra that the complex dissociates via very different pathways by surface collision versus collisions with gas atoms. The predominant dissociation pathway upon collisions with argon was the ejection of a single subunit with the monomeric and trimeric product ions retaining approximately the same number of charges. The monomer distribution is centered at a charge state of 8+, while the most intense trimer product ion is the 7+ charge state, a distribution of product ions that is very similar to the results previously reported by Robinson and coworkers. It is important to note that these products are not reflective of the subunit interactions that occur within the transthyretin complex, as dimers are considered the tetrameric building blocks due to extensive anti-parallel hydrogen bonding interactions between  $\beta$ -sheets in the monomer-monomer interface of each subcomplex.<sup>40</sup>

In contrast to the data obtained by collisions with gaseous Ar, a much broader monomer charge state distribution was formed by surface collision. In the latter case, the charge retained by the monomer ions was more proportional to their mass within the original tetramer. The most abundant peak in Fig. 1b corresponds to the 4+ monomer ion, implying the subunit retains approximately  $\frac{1}{4}$  of the charge from the original precursor ion, rather than carrying out over  $\frac{1}{2}$  of the charge as in Fig 1a. As stated above, the charge state of the dissociating subunit is indicative of its conformation. The high charge state observed by dissociation through argon collisions implies the ejected monomer has undergone extensive unfolding prior to ejection from the complex. Likewise, it is proposed that the low monomer charge states observed by surface collision suggest a more folded monomer conformation upon dissociation from the complex. The trimeric product ions generated by surface collision also retain an amount of charge that is proportional to their mass. These ions carry an increased number of charges relative to those produced by gaseous collisions, with the 11+ trimer retaining about 75% of the precursor ion charge. In addition to monomers and trimers, dimeric product ions are also present following surface collision. While a minor amount of dimer is observed by CID, up to eight dimeric charge states are observed following collision with the surface. Here both the mass and charge of the complex is split nearly symmetrically. Again, the significance of this is that the basic unit of structure is believed to be dimeric.<sup>40</sup> Even in the case of surface collision however, the dimeric product ions are still present in much lower abundance than monomeric and trimeric ions. Due to the homo-oligomeric nature of this complex, charge states for several of the product ions overlap in  $m/z$  ratio, thus it is difficult to estimate of the exact percentage of dimer, i.e. the 7+ dimer overlaps in  $m/z$  ratio with the 14+ tetramer.

In attempt to resolve overlapping product ions and gain a clearer picture of the oligomers generated by surface collision, a theoretical deconvolution of the experimental SID spectrum



was performed by simulating individual charge state envelopes for each oligomeric product. Starting with the monomer population, each individual peak was modeled using a three point Gaussian curve based on the  $m/z$  ratio, intensity, and width of each peak from the experimental spectrum. Dimer and trimer populations were simulated in the same manner, while only two peaks were modeled for the tetramer population, the isolated precursor ion and one adjacent charge state representing the loss of a single positively charged solvent adduct, a common observation in the dissociation of non-covalent protein complexes.<sup>39</sup> In cases where experimental peaks could be comprised of different oligomers with overlapping  $m/z$  values, the contribution of each oligomeric species to the overall intensity of the peak was estimated by assuming a Gaussian distribution for the charge state population of each oligomer.

Figure 2 shows the deconvoluted spectra for each oligomer present in the SID spectrum (monomer:red, dimer:green, trimer:blue, tetramer:purple). The sum of these simulated spectra are shown at the top of Figure 2 in orange and overlaid by the experimental spectrum in black. The total simulated spectrum is a close representation of the experimental data. While the simulated charge state envelopes of the dimer and trimer ions have a near Gaussian distribution, the monomer population appears to have two separate charge state envelopes, one centered around the 7+ charge state and the other around the 4+/5+ charge state. The non-Gaussian behavior of the monomer distribution is likely due to the presence of different subunit conformations within the population, however, further dissociation of the primary dimer/trimer fragment ions cannot be ruled out. The higher charge states represent an unfolded conformation as observed in the case of gaseous collisions, while the lower charge states corresponding to a more folded subunit. This suggestion is supported by the fact that the relative intensity of the lower charge states increases at higher surface collision energies (see below). It becomes evident from the simulated spectra that the 15+ tetramer dissociates primarily into a monomer with 5 charges and trimer with 10 charges, or a complementary pair of dimers with 7 and 8 charges (shown with brackets in Figure 2). This signifies a much more even split of the tetramer than that produced by argon collisions, and slightly more representative of the dimeric substructure of transthyretin.

The dissociation characteristics of transthyretin were further considered by accelerating the tetrameric ions into the surface over a wide range of kinetic energies. Surface-induced dissociation spectra for the 15+ transthyretin tetramer as a function of increasing collision energy are displayed in Figure 3(a–c) and demonstrate that the observed dissociation products are affected by the collision energy that is employed. Comparison of all three spectra shown in this figure reveals that monomers are ejected with a lower number of charges as the collision energy increases. The lowest collision energy (Figure 3a) was acquired at a DC offset of 30 volts between the source hexapole and the surface ( $\Delta V = 30$  V, corresponding to a collision energy of 450 eV once corrected for the 15+ precursor ion charge state). At this energy, the most abundant ions are tetramers that have not dissociated after collision with the surface. There are however, a low abundance of monomeric and trimeric product ions observed. The most intense monomer peak corresponds to the 8+ charge state, while the most abundant trimer is the 7+ product ion. Therefore, as observed by gaseous collisions in Figure 1a, the favored monomer product ion carries approximately one-half of the available protons. This is dramatically different from the surface collision spectrum shown in Figure 1b which was collected at a collision energy of 750 eV. At even higher collision energies (Figure 3b, 3c) the product ions are predominantly monomers centered about the 4+ charge state, which represents a nearly symmetric split of charges with respect to the relative mass of an individual subunit (1/4 of the precursor ion). Consequently, while low energy surface collisions yield highly charged monomer and complementary trimer ions, high energy collisions of transthyretin predominantly generate monomers with a low charge state. Collisions with argon, even at energies as high as 3000 eV (i.e. 200 V DC

offset, data not shown) always resulted in highly charged monomer product ions and the 4+ monomer ion was never observed.

In addition to differences in the product ions generated, it was observed that the dissociation of the tetrameric precursor ions could be achieved at much lower laboratory collision energies when a surface was employed as the collision target. This difference is clearly illustrated by plotting the decay of tetramer ion intensity as a function of collision energy for both gas and surface collisions (see Supplemental Information, Figure S1). The point corresponding to approximately 50% depletion of the tetramer occurs at approximately 400 eV lower when transthyretin is collided into a surface, despite the fact that the gas pressures used in these CID experiments predict around 4,000 collisions with argon.<sup>41</sup>

Figure 4 illustrates plausible pathways that may lead to the product ions observed and help shed light on the differences between gaseous and surface collisions. As was shown in Figure 1 and in multiple publications,<sup>41–43</sup> collisions of non-covalent protein complexes with gas atoms leads to dissociation pathways that are asymmetric with respect to both mass and charge. To explain the monomer charge enrichment that is typically observed it has been proposed by numerous research groups that significant unfolding of the ejected subunit must occur allowing charge to be redistributed in a Coulombically favorable manner proportional to the surface areas of the unfolded monomer and complementary (n-1)-mer.<sup>23–26</sup> This can be rationalized, in part, because internal energy is added incrementally via multiple low-energy collisions with small inert gas atoms or molecules. The activation time frame for CID of transthyretin is on the order of a few hundred microseconds.<sup>41</sup> During this gradual activation it may be possible to disrupt the structure of a protein complex initiating unfolding of a monomer with only a small fraction of the collisions that are ultimately required for dissociation. Although this is shown in Figure 4 as the initial barrier along the reaction pathway that must occur prior to the dissociation event, it is feasible that multiple unfolding transitions occur. Clemmer and coworkers previously reported the possibility of multiple protein unfolding transitions in a study of cytochrome *c* monomers stored in an ion trap prior to an ion mobility experiment.<sup>44</sup> It is likely, however, that once a monomer begins to unfold, further unfolding of that monomer is a cooperative lower energy process than unfolding of other still-folded monomers. Evidence of this comes from observations made during the force-induced unfolding of multi-domain proteins. For example, mechanical unraveling of tandem immunoglobulin domains in the protein titin by atomic force microscopy (AFM) results in successive rather than simultaneous unfolding of the individual domains.<sup>45, 46</sup>

Given the makeup of subunit interfaces, it is possible to envision a scenario during the CID activation process in which the internal energy of the protein is only sufficient enough to destabilize a fraction of the non-covalent bonds between the leaving subunit and the rest of the complex. A systematic analysis of oligomeric proteins ranging from dimers to octamers revealed that the subunit interface area for such complexes can range from approximately 700 to over 10,000 Å<sup>2</sup> per subunit.<sup>47</sup> Oligomers with interfacial surface areas above 1500 Å<sup>2</sup> per subunit contained, on average, 1 intermolecular hydrogen bond per every 200 Å<sup>2</sup>, implying a single subunit can contain as many as tens of hydrogen bonds to the rest of the complex. In addition, much of the inter-subunit surface area is dominated by hydrophobic side chains (~65% nonpolar on average), but also contains a large number of charged residues. After leucine, arginine residues were found to make the most prevalent contribution to inter-subunit surface area, implying a significant enrichment of both salt-bridges and hydrophobic interactions when compared to the non-interfacial regions of oligomeric proteins. The fact that each subunit interacts with the rest of the protein through multiple sites suggests that each successive gas collision may disrupt some of the inter-subunit bonds, but allow other interactions in the subunit interface to remain intact, or even

form bonds at new sites. Simultaneously, intramolecular non-covalent bonds may also break, leading to an extended subunit “clinging” to the remainder of the complex.

The SID process on the other hand, is a sudden, single-step activation. While this does not necessarily imply a single solitary collision or contact point (in fact it is very likely the complex makes contact with the surface at multiple positions, or possibly even rolls across the face of the surface) the residence time of the ion at the surface is likely on the order of picoseconds.<sup>48–50</sup> The dissociation event itself may occur on a longer timescale, but, the ion excitation step depicted on the right-hand side of Figure 4 occurs in a brief period of time relative to multiple collisions with argon. We propose that this process is sufficiently rapid and energetic to facilitate the rupture of multiple intermolecular bonds between subunits prior to large scale structural rearrangement of a single monomer. Product ions generated via surface collisions should therefore have a more compact or “folded” structure than those produced by gaseous collisions. The notion that structural similarity between subunits would be reflected by their charge symmetry is supported by the observation of symmetrically charged product ions in the CID spectra of denatured protein/peptide aggregates.<sup>24, 51</sup> In these cases, however, the interacting monomers have lost their native structure prior to gas-phase activation, and the symmetrically charged product ions result from the lack of disproportionate charge transfer between subunits that are highly unfolded.

From Figure 1, it also appears that product ions other than monomers and (n-1)-mers could be produced by such a mechanism. If the SID collision energy is too low to break the numerous non-covalent attachments of a subunit or subunits to the remainder of the complex, unfolding can occur producing a spectrum similar to that of CID (compare Figure 1a and 3a). This again parallels the mechanical resistance of proteins studied by AFM in which the simultaneous rupture of multiple bonds requires greater force than the sequential breaking of single bonds<sup>46, 52</sup>.

### Probing Monomer Unfolding by In-Source Activation Prior to SID

In order to test the hypothesis that product ions generated by surface collision are more compact than those produced through gas collisions, we investigated the influence of protein conformation on the dissociation products observed in each case. In the Q-TOF 2 instrument employed for these studies, it is possible to either preserve or activate/dissociate protein complexes by using gentle or harsh voltages, respectively, in the initial source regions of the instrument. It has been demonstrated that protein complexes dissociate through the same subunit unfolding mechanism, whether they are activated through multiple argon collisions in the gas cell or through collisions with air in the source.<sup>26</sup> Ruotolo et al. applied ion mobility measurements to source-activated macromolecular complexes, demonstrating that by monitoring protein conformation in the gas-phase, unfolded (but intact) protein intermediates can be observed long after source activation.<sup>53</sup> Here, we varied the source voltages to compare the surface collision of a partially unfolded intermediate produced under harsh source conditions versus that of a more “native-like” conformation preserved under more gentle source conditions.

We examined hemoglobin, a heterotetramer composed of two pairs of hemecontaining alpha- and beta-subunits. Each subunit weighs just under 16 kDa (minus the heme), making the intact complex approximately 12 kDa larger than the TTR tetramer. Also like the TTR tetramer, human hemoglobin exhibits a dimeric substructure, with  $\alpha\beta$  dimers existing in equilibrium with the tetrameric form.<sup>54</sup> Figure 5 is a comparison of dissociation spectra for tetrameric human hemoglobin acquired by gaseous and surface collisions under identical source conditions and laboratory collision energies. Collision of the 17+ tetramer with argon (Figure 5a) causes the typical ejection of highly charged monomers along with trimeric product ions that carry the remainder of charge. As hemoglobin is a heterotetramer, either



the alpha- or beta-subunit can be ejected from the precursor ion, and both monomers are observed in the product ion spectrum, with the  $\alpha/\beta$  ratio varying from experiment to experiment. Trimeric product ions corresponding to  $2\alpha$ -plus one  $\beta$ -subunit and  $2\beta$ - plus one  $\alpha$ -subunit are observed, with varying numbers of non-covalently bound heme groups attached to each. The inset of Figure 5 shows an expansion of the  $m/z$  region containing the  $10+$  trimeric products in which each of the ions in this complex mixture can be resolved.

Figure 5b shows SID of the  $17+$  tetramer acquired at the same collision energy as the spectrum in Figure 5a. At this particular collision energy, the product ions are almost entirely monomeric, consistent with dissociation not to monomer plus trimer but mainly to four monomers. The higher abundance of  $\alpha$  and the variability in the  $\alpha/\beta$  ratio from experiment to experiment in both CID and SID is not yet fully understood because even dissociation of  $\alpha\beta$  dimer produces more abundant  $\alpha$  peaks. The charge state distribution of the monomers generated by SID is shifted up in  $m/z$  toward lower charge states, as was the case for SID-generated monomers of TTR at higher collision energies, indicating a more folded conformation. Significantly, the monomer ions that retain the least amount of charge (i.e. the  $3+$  and  $4+$  alpha subunit) and likely correspond to the most compact conformations, also exhibit some retention of the non-covalently bound heme group. This observation supports the hypothesis that surface-induced dissociation precedes significant structural rearrangement, and suggests that elements of the native monomer tertiary structure are conserved following dissociation.

Dissociation of the  $17+$  tetramer was then examined as a function of increasing cone voltage in the ion source to promote partial protein unfolding prior to mass selection and dissociation. The cone voltage was varied from 40 to 120 volts, allowing the protein to undergo more energetic collisions with air molecules in the rough vacuum of the source region at higher cone voltages. Lower cone voltages help to better preserve the intact complex, while higher cone voltages serve to activate and partially unfold the protein. In-source activation of hemoglobin followed by ion mobility-MS experiments have been performed to confirm that the ion's collision cross-section does indeed increase due to unfolding at high cone voltages (see Supporting Information, Figure S2). The energized, and likely partially unfolded,  $17+$  tetramer was then selected with the quadrupole mass analyzer and subjected to collisions with argon in the gas cell or collision with the fluorinated SAM film to explore the effects of protein conformation on ion-surface collisions. The left-hand column of Figure 6 shows an expanded view of the low  $m/z$  region to demonstrate the effect of increasing cone voltage on the CID spectra of hemoglobin. Regardless of how harsh the source conditions are, subsequent 1190 eV collisions with argon in the hexapole collision cell result in the ejection of a highly charged monomeric subunit, centered about the  $9+$  alpha-subunit. The right-hand column of Figure 6 (d-f) shows the results of colliding with the surface at 1190 eV, with ions produced initially at the same three source voltages used for source activation prior to CID (Figure 6 a-c). Unlike the CID product ions, the charge state distribution of monomeric products observed in the SID spectra changes with cone voltage. When a source voltage of 40 volts is employed (Figure 6d), the  $5+$  alpha-subunit is the most abundant monomer charge state, as was the case in Figure 5b. As the cone voltage is increased to 80 and 120 volts (Figure 6e and 6f, respectively), and the conformation of the selected precursor (activated in the ion source) presumably becomes more unfolded, the charge state distribution shifts such that the  $6+$  and  $7+$  alpha subunits, respectively, become the most abundant. In addition, the  $9+$  alpha-subunit is also now observed at the two higher cone voltages. The SID results illustrate that denaturation of the tetramer through collision with air molecules in the source region generates an unfolded conformation prior to surface collision. In this scenario, charge transfer to a partially unfolded monomer may occur before the complex even comes into contact with the surface, resulting in more highly charged monomers at higher cone voltages. This suggests that the dissociation products that result

from surface collision are highly sensitive to the conformation of the protein that strikes the surface.

### CID vs. SID of Pentameric C-Reactive Protein

To further investigate the influence of subunit number on the dissociation of oligomeric proteins, the pentamer of C-reactive protein (CRP) was explored (see Supplemental Information, Figure S3). Each monomer has a molecular weight of approximately 23 kDa, giving the intact pentamer a mass of 115 kDa. Preservation of the intact pentamer of CRP, and pentamers of the closely related serum amyloid P component, within a mass spectrometer, has previously been reported by Aquilina and Robinson.<sup>55</sup>

Gaseous collisions of the 26+ pentamer once again result in a highly charged monomer and (n-1)-mer, or tetramer in this case, with the ejected subunit taking out a little less than half the precursor charge. Surface collision of CRP yields only monomeric fragment ions that contain approximately 1/5 of the charge from the 26+ precursor ion, indicating the homopentamer dissociates into five nearly charge-equivalent monomers. In addition, the charge state distribution is relatively narrow, with mainly 5<sup>+</sup> to 7<sup>+</sup> charge states observed by SID, as compared to 9 monomeric charge states observed by CID (5+ to 13+, with 11+ most abundant).

Energy-resolved SID of the 26+ CRP pentamer (see Supplemental Information, Figure S4) reveals the presence of only monomeric product ions with a charge percentage approximately equivalent to their mass percentage (i.e. about 20%) across all energies explored. For all SID collision energies, there is no intact CRP pentamer left even after the lowest energy surface collision, and collision conditions soft enough to retain some of the 26+ precursor ion could not be achieved in this experiment. This may be a reflection of the structural interaction between subunits within the CRP pentamer. The inter-subunit contacts in CRP consist mainly of salt bridges in the loop spanning from residues 115–123 on one subunit to a variety of residues in the next subunit.<sup>56</sup> This is in contrast to other systems in which there are often inter-subunit  $\beta$ -sheets or domain-swapped regions. The facile surface-induced dissociation of this complex may be related to the lack of interfacial surface area between subunits, a prospect that is under further investigation. Because of their different energy input pathways and different energy levels achieved, CID and SID may also sample and fragment different precursor ion populations. For CRP, for example, low SID energies produce mainly 5<sup>+</sup> and 6<sup>+</sup> monomers while higher SID energies yield 4<sup>+</sup>, 5<sup>+</sup>, 6<sup>+</sup>, and 7<sup>+</sup>. If the entire population consists of a distribution of different charge distributions, with 26 charges distributed over 5 subunits in different ways (e.g., [5,5,5,5,6] plus [4,5,5,6,6] plus [4,5,5,5,7]), the lowest energies may access dissociation only from the dominant most symmetrical charge distribution [5,5,5,5,6] population while higher energies also fragment [4,5,5,6,6] and [4,5,5,5,7]. Recent theoretical studies on the dissociation of protein complexes conducted by Wanasundara and Thachuk predict an energetically favorable symmetric partitioning of charge between two product ions of equal surface area.<sup>27</sup> For complexes dissociated by CID, this means that the unfolded monomer and (n-1)-mer split the overall charge approximately equally as the two fragments often possess roughly equivalent surface areas. This Coulomb repulsion model also predicts however, that if dissociation can be achieved on a time-scale that is fast as compared to protein conformational changes, that “monomers ejected from an n-mer would be expected to carry a charge of approximately 1/n of the total charge on the complex.” This is shown graphically in Figure 7, where the black bars represent the theoretical percentage of charge expected if a “native” monomer dissociated from each of the proteins examined in this study, along with charge state statistics for two previously published protein CID/SID comparisons.<sup>36, 38</sup> The conformation of the dissociated monomers can be assessed experimentally by considering

the average charge state (A.C.S.) of the ejected subunits, as calculated by the following expression:

$$\text{A.C.S.} = \sum I_s z_s / \sum I_s \quad (1)$$

where  $I_s$  is the intensity of monomer product ions in the experimental spectrum, and  $z_s$  is the charge state of each product ion. The average charge state experimentally observed for monomers dissociated through argon collisions (white bars) and surface collision (gray bars) is shown as a percentage of the original charge on the protein complex. In each case, CID (white bars) results in monomer ions that carry away nearly 50% of the charge even though the monomer mass is only 20–25% of the total mass, representing an unfolded monomer population. At sufficiently high collision energies however, monomer ions generated through surface collision approach the theoretical charge state expected if the original conformation of the subunit is preserved upon dissociation (gray bars vs. black bars). Slight discrepancies between the theoretical average charge state and that one measured via surface collision may be due to the presence of competitive dissociation pathways that produce charge enriched monomer product ions as well as more folded monomer products. Still, the theoretical predictions are in good agreement with what is observed experimentally by the fast, energy-sudden surface activation of protein complexes at sufficiently high energies. Dissociation of each complex at sufficiently high energy leads to predominantly monomeric product ions with a nearly even partitioning of the overall charge. These results, when viewed in context of the Coulomb repulsion model, add support to the notion that surface collisions can provide access to structurally informative dissociation pathways.

## Conclusions

This study presents fundamental differences in the dissociation of non-covalent assemblies of proteins when collided into a surface versus small gas atoms. For each complex investigated, the products of surface collision retained charge that was more consistent with their mass contribution in the overall complex. Provided the collision energy was sufficiently high, SID resulted in fragmentation into primarily monomeric product ions with the charge being nearly evenly distributed among the monomers. We propose this is due to the rapid, high energy deposition provided by surface collisions, and attribute the more symmetric distribution of charge to the conformation of the protein subunits upon dissociation. A consequence of the fast activation is that protein subunits are free to dissociate prior to large scale structural rearrangement of the individual subunits. This leads to product ions that may retain much of their original conformation and consequently even some of their non-covalent contacts within the assembly. This is supported by the fact that subunit unfolding prior to surface collision influences the charge partitioning among the subunits and that less unfolded (lower charge) monomers retain non-covalent heme ligands. In addition, energy-resolved SID of TTR revealed that monomeric product ions decrease in charge at higher collision energies, emphasizing the necessity for energy deposition to be both fast and sufficiently high to access dissociation pathways that precede unfolding.

The fact that alternative dissociation mechanisms exist for non-covalent protein complexes is enticing from a biological standpoint. The ability to derive structural information about the interaction and arrangement of subunits based on their gas-phase dissociation from the intact complex would greatly facilitate the rapid analysis of a wide variety of protein assemblies. While some of this information, such as the identification of the peripheral subunits in a hetero-oligomeric complex, can be determined through multiple collisions with gas, this methodology is still rather limited due to the ejection of only unfolded monomers. The ability to offer complementary or even more revealing structural details through surface

collision could add depth to the increasing power of mass spectrometry in the structural biology field.

## Supplementary Material

Refer to Web version on PubMed Central for supplementary material.

## References

1. Svedberg T, Fahraeus R. *J. Am. Chem. Soc.* 1926; 48:430–438.
2. Baca M, Kent SBH. *J. Am. Chem. Soc.* 1992; 114:3992–3993.
3. Lightwahl KJ, Winger BE, Smith RD. *J. Am. Chem. Soc.* 1993; 115:5869–5870.
4. Loo JA. *J. Mass Spectrom.* 1995; 30:180–183.
5. Gavin AC, Aloy P, Grandi P, Krause R, Boesche M, Marzioch M, Rau C, Jensen LJ, Bastuck S, Dumpelfeld B, Edelmann A, Heurtier MA, Hoffman V, Hoefert C, Klein K, Hudak M, Michon AM, Schelder M, Schirle M, Remor M, Rudi T, Hooper S, Bauer A, Bouwmeester T, Casari G, Drewes G, Neubauer G, Rick JM, Kuster B, Bork P, Russell RB, Superti-Furga G. *Nature.* 2006; 440:631–636. [PubMed: 16429126]
6. Xie YM, Zhang J, Yin S, Loo JA. *J. Am. Chem. Soc.* 2006; 128:14432–14433. [PubMed: 17090006]
7. van Duijn E, Simmons DA, van den Heuvel RHH, Bakkes PJ, van Heerikhuizen H, Heeren RMA, Robinson CV, van der Vies SM, Heck AJR. *Journal of the American Chemical Society.* 2006; 128:4694–4702. [PubMed: 16594706]
8. Sobott F, Benesch JLP, Vierling E, Robinson CV. *J. Biol. Chem.* 2002; 277:38921–38929. [PubMed: 12138169]
9. van den Heuvel RHH, Gato S, Versluis C, Gerbaux P, Kleanthous C, Heck AJR. *Nucleic Acids Res.* 2005; 33
10. Rappsilber J, Siniosoglou S, Hurt EC, Mann M. *Anal. Chem.* 2000; 72:267–275. [PubMed: 10658319]
11. Sharon M, Taverner T, Ambroggio XI, Deshaies RJ, Robinson CV. *PLoS Biol.* 2006; 4:1314–1323.
12. Hernandez H, Dziembowski A, Taverner T, Seraphin B, Robinson CV. *EMBO Rep.* 2006; 7:605–610. [PubMed: 16729021]
13. Taverner T, Hernandez H, Sharon M, Ruotolo BT, Matak-Vinkovic D, Devos D, Russell RB, Robinson CV. *Acc. Chem. Res.* 2008; 41:617–627. [PubMed: 18314965]
14. McLuckey SA, Vanberkel GJ, Glish GL. *J. Am. Soc. Mass Spectrom.* 1992; 3:60–70.
15. Lancaster KS, An HJ, Li BS, Lebrilla CB. *Anal. Chem.* 2006; 78:4990–4997. [PubMed: 16841922]
16. Hunt DF, Yates JR, Shabanowitz J, Winston S, Hauer CR. *Proc. Natl. Acad. Sci. U. S. A.* 1986; 83:6233–6237. [PubMed: 3462691]
17. Lightwahl KJ, Schwartz BL, Smith RD. *J. Am. Chem. Soc.* 1994; 116:5271–5278.
18. Schwartz BL, Bruce JE, Anderson GA, Hofstadler SA, Rockwood AL, Smith RD, Chilkoti A, Stayton PS. *J. Am. Soc. Mass Spectrom.* 1995; 6:459–465.
19. van den Heuvel RHH, van Duijn E, Mazon H, Synowsky SA, Lorenzen K, Versluis C, Brouns SJJ, Langridge D, van der Oost J, Hoyes J, Heck AJR. *Anal. Chem.* 2006; 78:7473–7483. [PubMed: 17073415]
20. Chowdhury SK, Katta V, Chait BT. *J. Am. Chem. Soc.* 1990; 112:9013–9015.
21. Smith RD, Loo JA, Edmonds CG, Udseth HR. *Anal. Chem.* 1990; 62:693–698. [PubMed: 2327585]
22. Clemmer DE, Hudgins RR, Jarrold MF. *J. Am. Chem. Soc.* 1995; 117:10141–10142.
23. Felitsyn N, Kitova EN, Klassen JS. *Analytical Chemistry.* 2001; 73:4647–4661. [PubMed: 11605843]
24. Jurchen JC, Williams ER. *J. Am. Chem. Soc.* 2003; 125:2817–2826. [PubMed: 12603172]

25. Jurchen JC, Garcia DE, Williams ER. *J. Am. Soc. Mass Spectrom.* 2004; 15:1408–1415. [PubMed: 15465353]
26. Benesch JLP, Aquilina JA, Ruotolo BT, Sobott F, Robinson CV. *Chem. Biol.* 2006; 13:597–605. [PubMed: 16793517]
27. Wanasundara SN, Thachuk M. *J. Am. Soc. Mass Spectrom.* 2007; 18:2242–2253. [PubMed: 17977010]
28. Versluis C, van der Staaij A, Stokvis E, Heck AJR, de Craene B. *J. Am. Soc. Mass Spectrom.* 2001; 12:329–336. [PubMed: 11281608]
29. Sobott F, Robinson CV. *Int. J. Mass Spectrom.* 2004; 236:25–32.
30. Rostom AA, Fucini P, Benjamin DR, Juenemann R, Nierhause KH, Hartl UF, Dobson CM, Robinson CV. *Proc. Natl. Acad. Sci. U. S. A.* 2000; 97:5185–5190. [PubMed: 10805779]
31. Damoc E, Fraser CS, Zhou M, Videler H, Mayeur GL, Hershey JWB, Doudna JA, Robinson CV, Leary JA. *Molecular & Cellular Proteomics.* 2007; 6:1135–1146. [PubMed: 17322308]
32. Jones CM, Beardsley RL, Galhena AS, Dagan S, Cheng GL, Wysocki VH. *J. Am. Chem. Soc.* 2006; 128:15044–15045. [PubMed: 17117828]
33. Galhena AS, Dagan S, Jones CM, Beardsley RL, Wysocki VN. *Anal. Chem.* 2008; 80:1425–1436. [PubMed: 18247517]
34. Somogyi A, Kane TE, Ding JM, Wysocki VH. *J. Am. Chem. Soc.* 1993; 115:5275–5283.
35. Sobott F, Hernandez H, McCammon MG, Tito MA, Robinson CV. *Anal. Chem.* 2002; 74:1402–1407. [PubMed: 11922310]
36. Wysocki VH, Jones CM, Galhena AS, Blackwell AE. *J. Am. Soc. Mass Spectrom.* 2008; 19:903–913. [PubMed: 18598898]
37. Aquilina AJ, Benesch JLP, Bateman OA, Slingsby C, Robinson CV. *Proc. Natl. Acad. Sci. U. S. A.* 2003; 100:10611–10616. [PubMed: 12947045]
38. Wysocki VH, Joyce KE, Jones CM, Beardsley RL. *J. Am. Soc. Mass Spectrom.* 2008; 19:190–208. [PubMed: 18191578]
39. Sobott F, McCammon MG, Robinson CV. *Int. J. Mass Spectrom.* 2003; 230:193–200.
40. Blake CCF, Geisow MJ, Oatley SJ. *J. Mol. Biol.* 1978; 121:339–356. [PubMed: 671542]
41. Benesch JLP, Ruotolo BT, Simmons DA, Robinson CV. *Chem. Rev.* 2007; 107:3544–3567. [PubMed: 17649985]
42. Loo JA. *Int. J. Mass Spectrom.* 2000; 200:175–186.
43. Heck AJR, van den Heuvel RHH. *Mass Spectrom. Rev.* 2004; 23:368–389. [PubMed: 15264235]
44. Badman ER, Hoaglund-Hyzer CS, Clemmer DE. *Anal. Chem.* 2001; 73:6000–6007. [PubMed: 11791572]
45. Rief M, Gautel M, Oesterhelt F, Fernandez JM, Gaub HE. *Science.* 1997; 276:1109–1112. [PubMed: 9148804]
46. Brockwell DJ, Paci E, Zinober RC, Beddard GS, Olmsted PD, Smith DA, Perham RN, Radford SE. *Nature Structural Biology.* 2003; 10:872–872.
47. Janin J, Miller S, Chothia C. *J. Mol. Biol.* 1988; 204:155–164. [PubMed: 3216390]
48. Christen W, Even U, Raz T, Levine RD. *J. Chem. Phys.* 1998; 108:10262–10273.
49. Williams ER, Fang LL, Zare RN. *Int. J. Mass Spectrom. Ion Processes.* 1993; 123:233–241.
50. Meroueh O, Hase WL. *J. Am. Chem. Soc.* 2002; 124:1524–1531. [PubMed: 11841324]
51. Smith RD, Light-Wahl KJ, Winger BE, Loo JA. *Org. Mass Spectrom.* 1992; 27:811–821.
52. Kim T, Rhee A, Yip CM. *Journal of the American Chemical Society.* 2006; 128:5330–5331. [PubMed: 16620090]
53. Ruotolo BT, Hyung SJ, Robinson PM, Giles K, Bateman RH, Robinson CV. *Angew. Chem. Int. Edit.* 2007; 46:8001–8004.
54. Antonini E. *Science.* 1967; 158 1417-&.
55. Aquilina AJ, Robinson CV. *Biochem. J.* 2003; 375:323–328. [PubMed: 12892563]
56. Shrive AK, Cheetham GMT, Holden D, Myles DAA, Turnell WG, Volanakis JE, Pepys MB, Bloomer AC, Greenhough TJ. *Nat. Struct. Biol.* 1996; 3:346–354. [PubMed: 8599761]



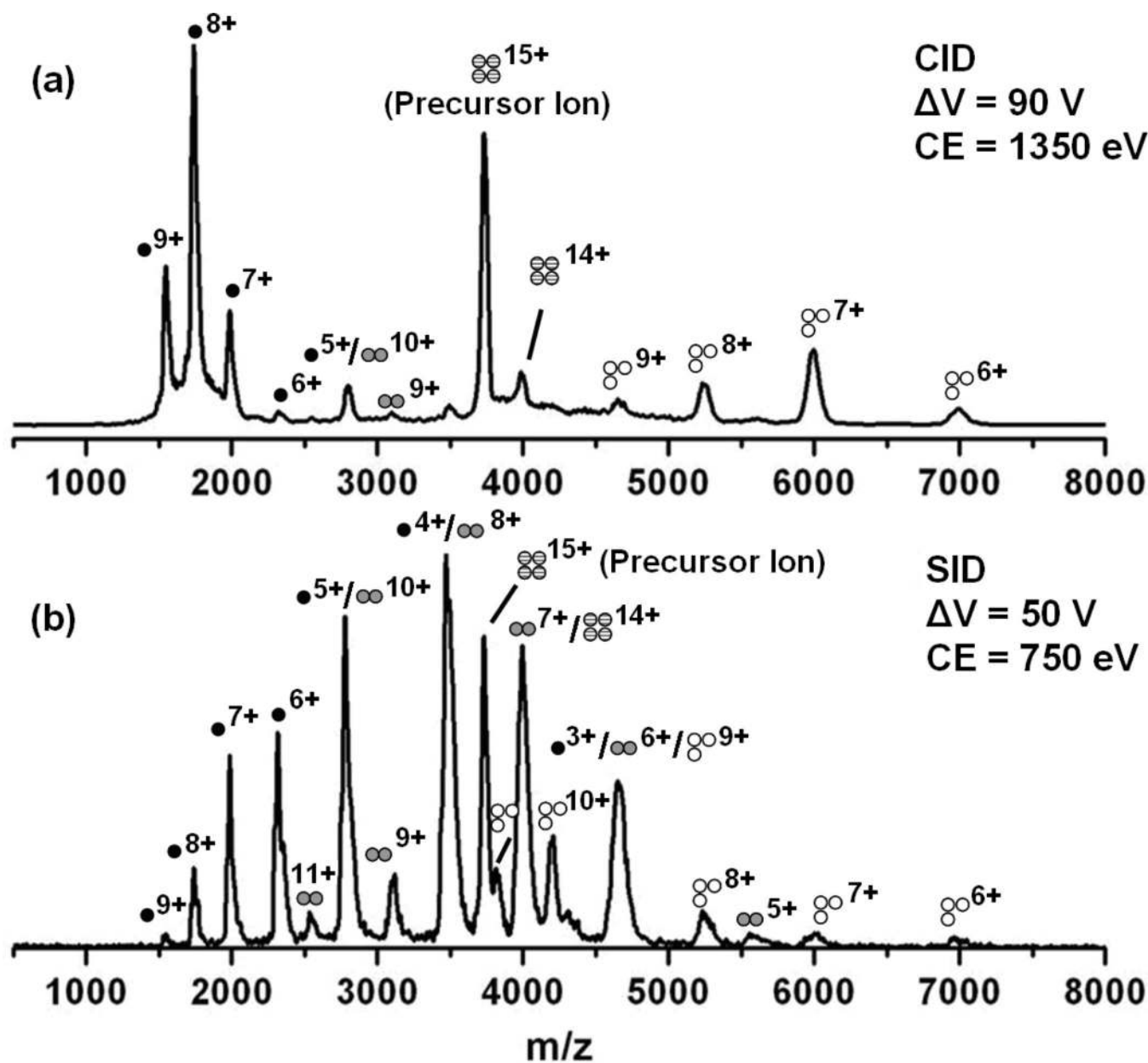


**Figure 1.** Dissociation of the 15+ charge state of homotetrameric transthyretin through collisions with argon atoms (a) and a fluorinated self-assembled monolayer on gold (b). Laboratory collision energies of 1350 eV and 750 eV were employed for gaseous and surface collisions, respectively. The product ions are labeled in each spectrum with colored circles: monomers are represented by a single black circle, dimers by two light gray circles, trimers by three white circles, and tetramers by four striped circles.

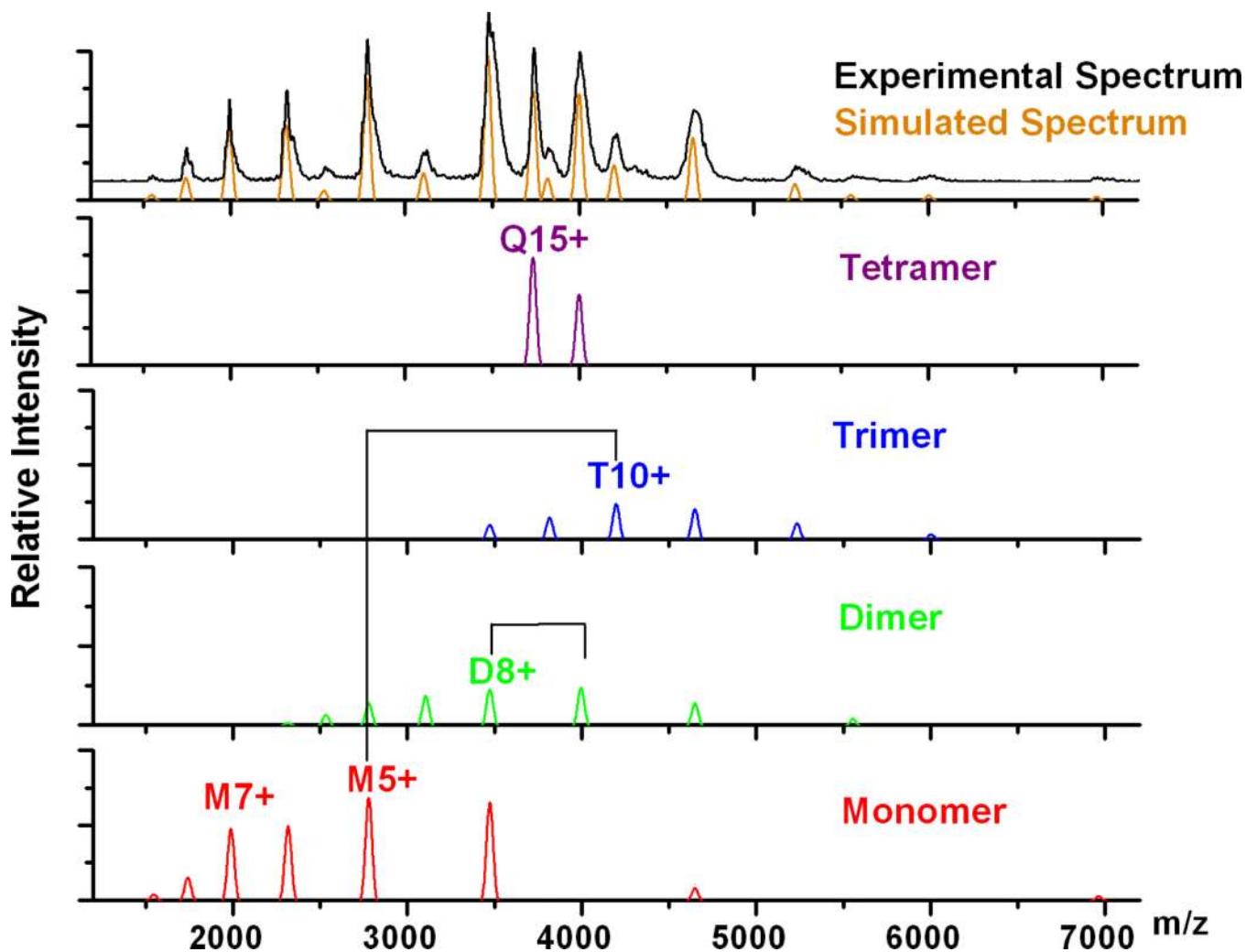


**Figure 2.** Theoretical deconvolution of the overlapping oligomeric fragment ions present in the SID spectrum of  $(\text{TTR})_4^{15+}$  shown in Fig. 1b. Spectra for each individual oligomeric species (monomer through tetramer) were simulated from the  $m/z$  values and intensities for the corresponding peaks in the experimental spectrum. It was assumed that each oligomer population would have a Gaussian distribution, with exception of the tetramer spectrum for which the precursor (15+) and one charge stripped ion (14+) were included. The orange spectrum at the top represents the sum of the simulated spectra and provides a close match to the experimental spectrum shown in black.

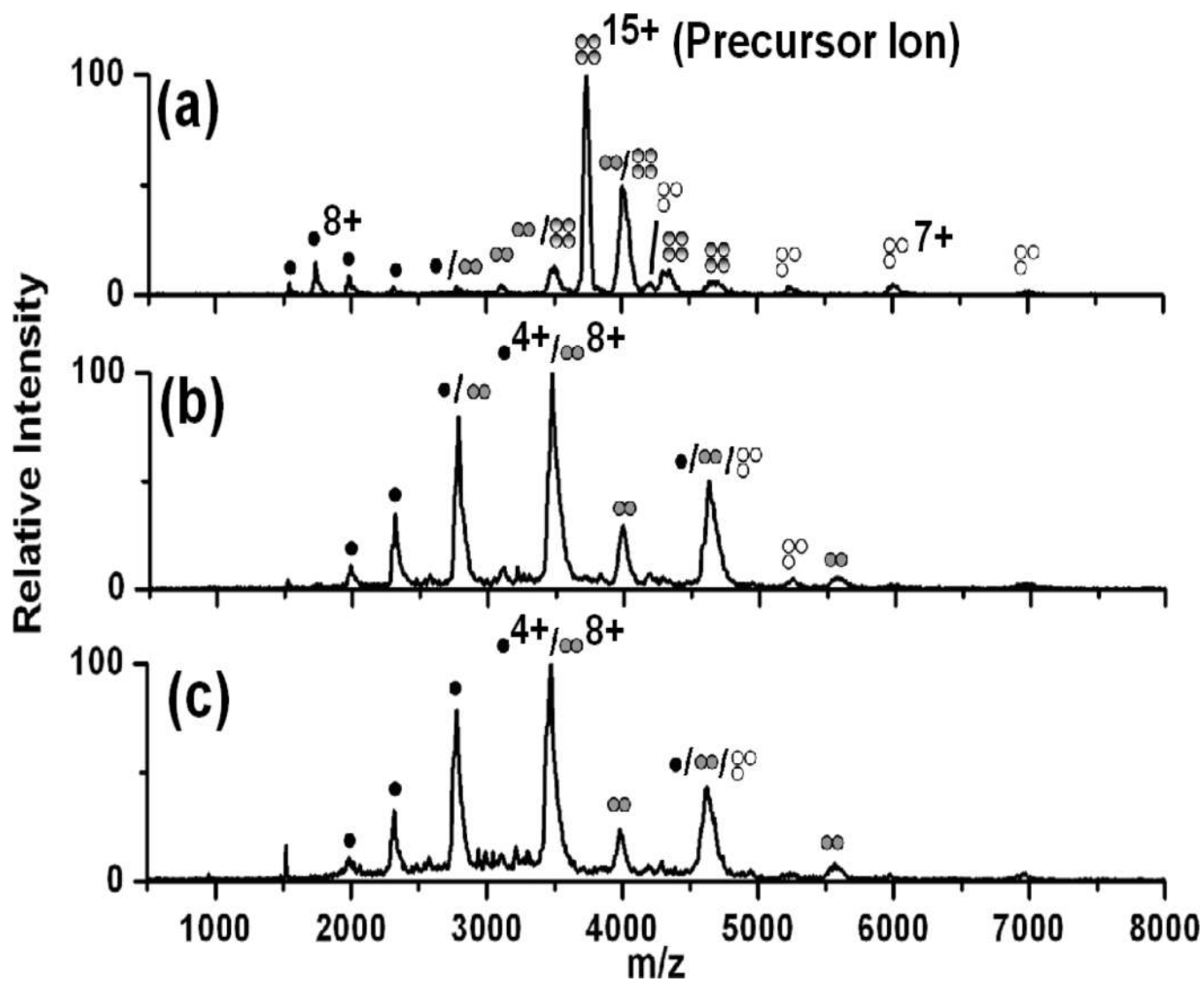


**Figure 3.** Energy resolved SID spectra of transthyretin at laboratory collision energies of (a) 450 eV,  $\Delta V = 30$  V; (b) 1050 eV,  $\Delta V = 70$  V; and (c) 1350 eV,  $\Delta V = 90$  V.

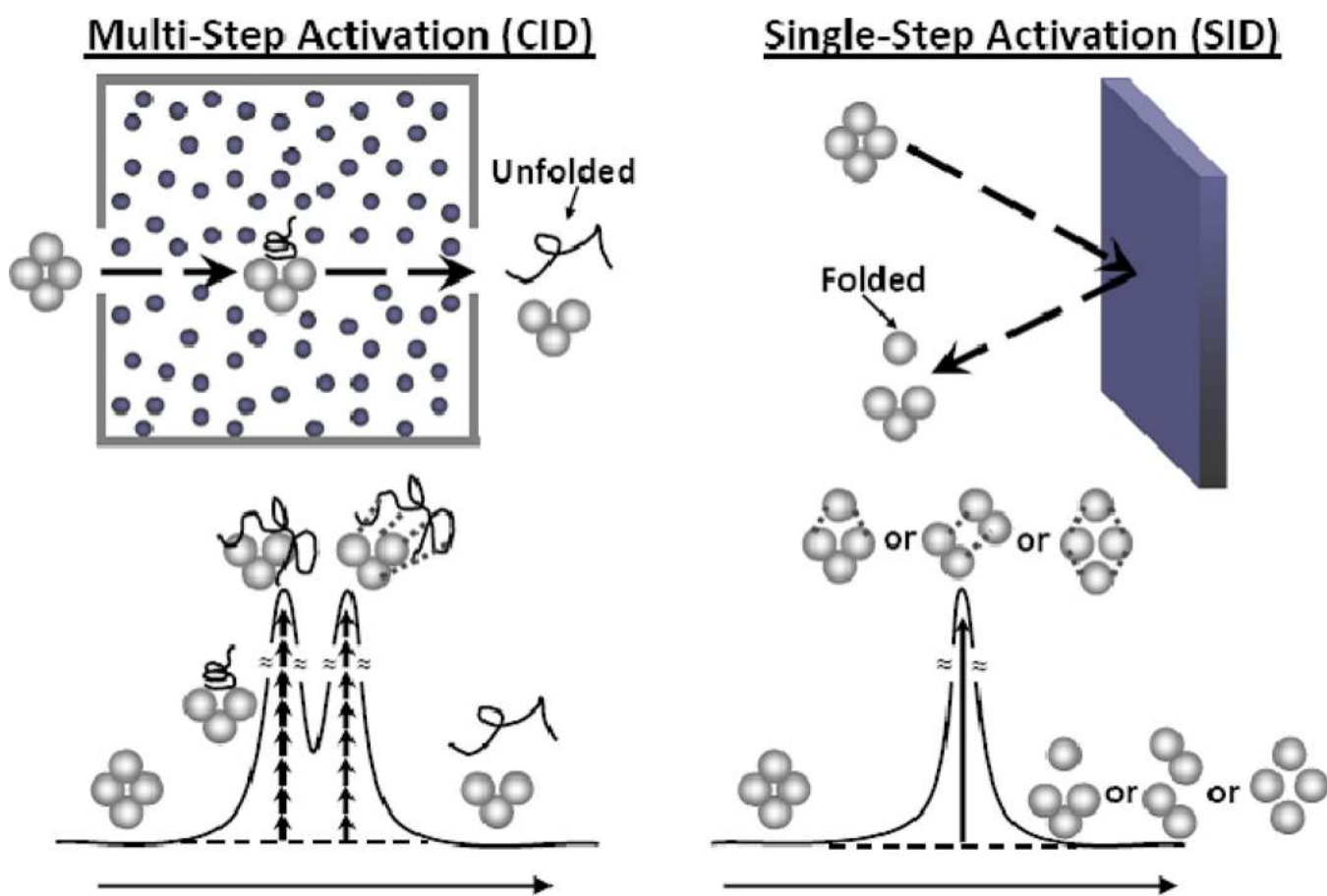


**Figure 4.** Schematic representation of the CID and SID experiments (top) and simplified reaction pathway for dissociation of a non-covalent protein complex via CID or SID (bottom, with reaction coordinate on the x-axis and energy on the y-axis; actual energies needed and achieved, and numbers of rearrangements/non-covalent bonds broken, are unknown). In CID, multi-step activation with gas atoms causes structural rearrangement (isomerization) resulting in the ejection of an unfolded subunit. In SID, rapid energy deposition through surface collision is proposed to induce dissociation prior to significant protein structural rearrangements leading to alternative dissociation channels. Differences in products achieved with different energy input and different dissociation time frames has been observed for decades, even for relatively small molecules, when structures are capable of isomerizing and fragmenting via isomer or original structure.

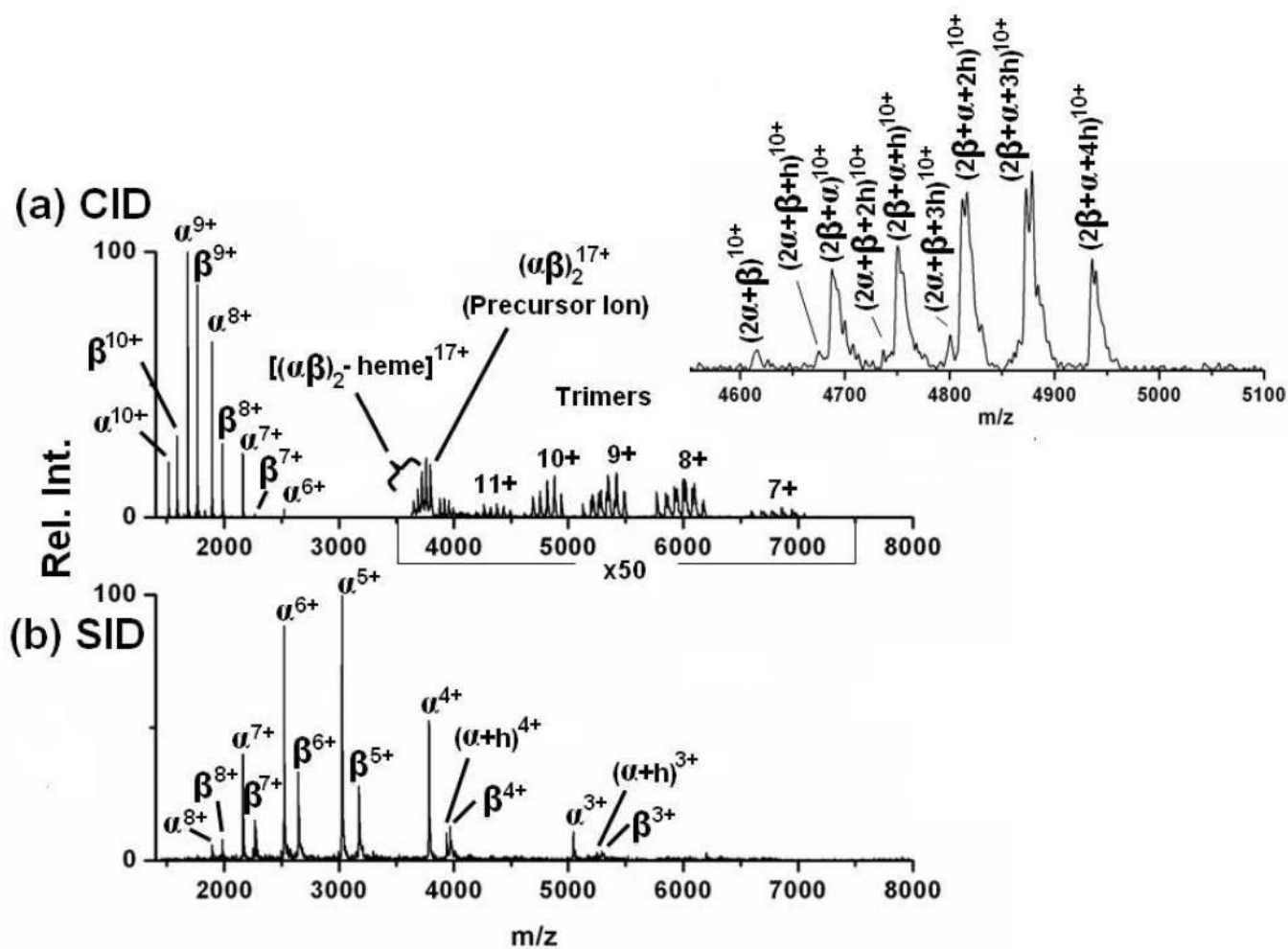


**Figure 5.** Comparison of CID (a) and SID (b) spectra for the 17+ tetramer of human hemoglobin at a collision energy of 1190 eV. Inset is an expansion of the trimeric product ion mixture of heme,  $\alpha$ -, and  $\beta$ -subunits for the 10+ charge state observed by CID.



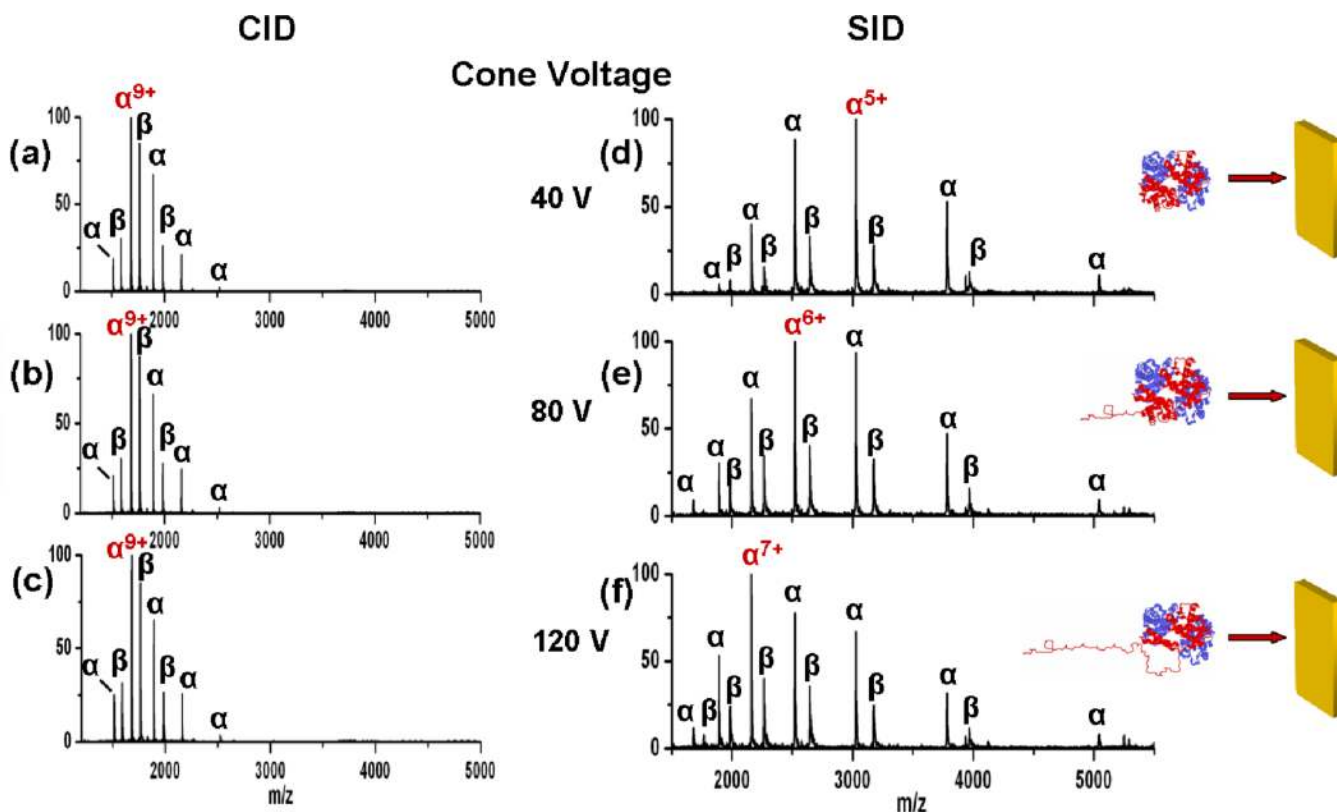


**Figure 6.**

In-source activation of human hemoglobin followed by selection of the 17+ tetramer and dissociation by CID (a–c) or SID (d–f). At cone voltage of 40 V (a, d), a more folded conformation of hemoglobin is selected for dissociation. Higher cone voltages (b–c, e–f) can promote partial subunit unfolding in the source prior to mass selection and true MS/MS. While the denaturation has virtually no effect on the CID products at 1190 eV collision energy, the charge state of the monomers generated by SID at the same energy increases with increasing cone voltage, indicating the dissociation products are sensitive to the conformation of the protein that collides into the surface.

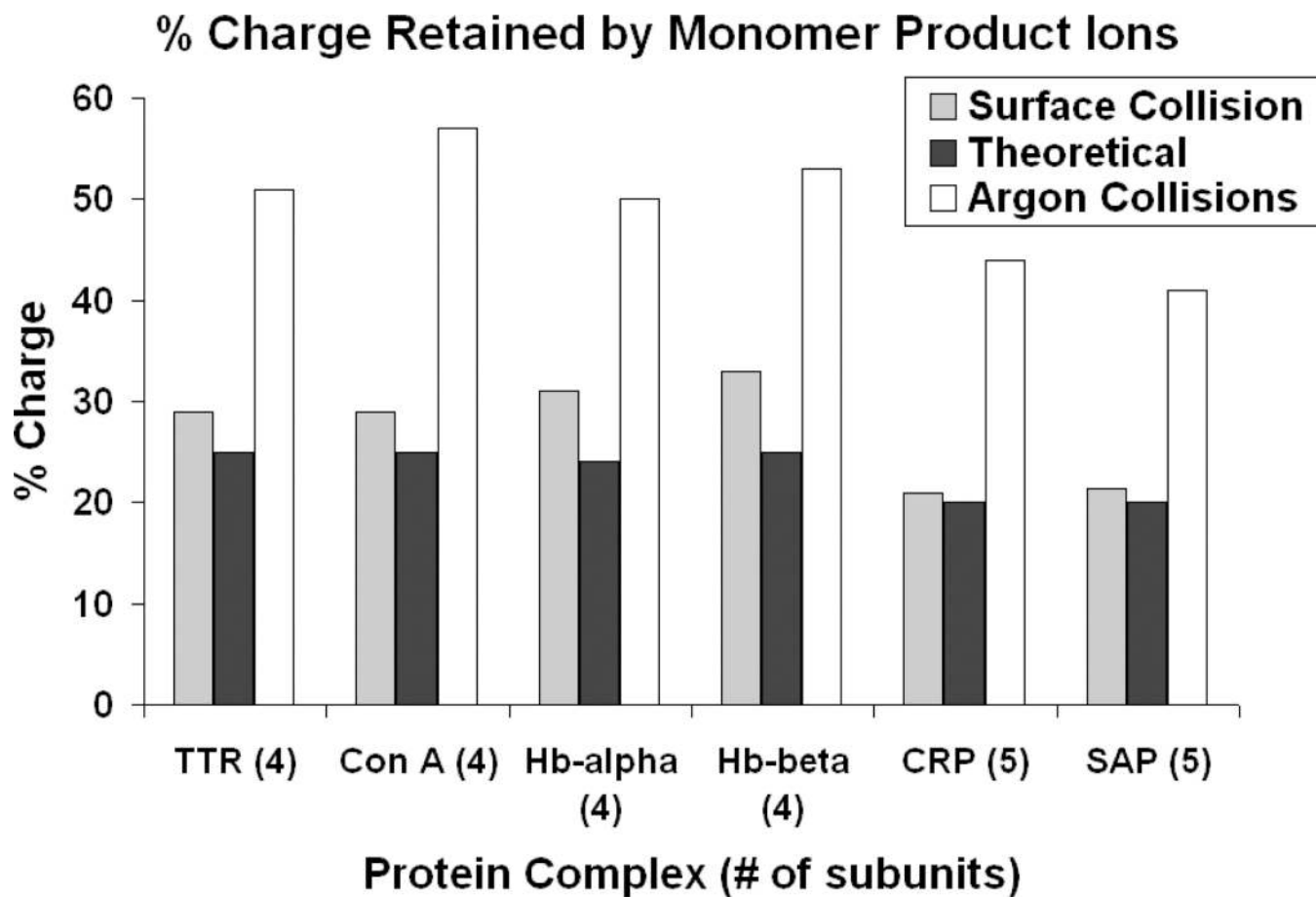


**Figure 7.**

Percentage of charge from the original protein complex that is retained by monomer ions dissociated from tetramers and pentamers through argon collisions (white) and surface collision (gray). The theoretical percentage (black) represents the amount of charge expected to be retained if monomers simply share the charge of the complex equally.